# Explosive acceleration of fluoropolymerbased reactive material fragments

<u>Hayleigh J. Lloyd</u>, Denise Meuken, Martijn Zebregs, Michael Y. K. Hu, Richard H. B. Bouma

TNO, Ypenburgse Boslaan 2, 2496 ZA, The Hague, The Netherlands.

Hayleigh.lloyd@tno.nl

#### Abstract

Energetic materials that contain metal and metal oxide powders, fluoropolymers and fillings are classed as reactive materials. Fragments from these materials may release significant amounts of energy upon impact when surviving mechanical loads during acceleration and flight, resulting in intensified damage effects to the target. Composites were prepared into reactive fragments using alternative fabrication techniques to achieve functional fragments that have the potential to be scaled up. The fragment preparation as well as the successful projection of reactive material fragments from a 0.5" calibre gun on a target plate assembly and the registration of their reaction by high speed video was presented in [1].

Here results from the explosive acceleration of reactive fragments are presented. Two set-ups were designed aiming for fragment velocities of 1.0 and 1.5 km/s, with the reactive fragments encapsulated in a polymeric layer. The 1.0 km/s impact velocity was chosen for comparison to the previous gun launch projected fragments. The mechanical loads during acceleration by the detonating explosive, however, will be larger. With each experiment the effect of the reactive material fragments impact on a target plate assembly can be compared to the impact of inert aluminium fragments. It was found that some of the fragments were able to reach the target plate assembly, penetrate the first aluminium plate and react upon impact at the second plate.

#### 1. Introduction

Reactive materials, unlike traditional explosives and propellants, may display adequate insensitivity to common initiation methods and external stimuli. However, when subjected to high strain-rate loading, they react vigorously, releasing significant amounts of chemical energy. Among the various types of reactive materials are intermetallics, thermites, and metal-polymer mixtures, each differing significantly in reaction mechanisms, energy release, and preparation methods [2]. In recent years, a particular focus has been placed on metal-polymer mixtures, specifically metal-fluoropolymer materials.

One of the primary applications of reactive materials lies in the design and optimization of energetic fragments. By tailoring the properties of reactive materials, there is an aim to maximize the lethality, effectiveness, and safety of these weapons systems. Energetic fragments are designed to remain intact during acceleration, penetrate targets, and induce secondary reactions upon impact. Understanding the behaviour, properties, and mechanisms governing energetic fragments is essential for enhancing safety, optimizing performance, and advancing technological capabilities across multiple domains.

The study of energetic fragments encompasses a broad range of topics, including their composition, structure, velocity, trajectory, penetration capabilities, and secondary reaction mechanisms. Additionally, efforts are made to develop predictive models, simulation techniques, and experimental methodologies to better understand and quantify the behaviour of reactive fragments under different scenarios [3-8].

In previous work by the authors, an alternative preparation technique to create reactive materials was explored which has the potential to be scaled up [1]. The chosen reactive material composition comprised of aluminium, bismuth oxide and fluoropolymers. These fragments, when projected from a gun, remained intact beyond velocities of 1.0 km/s. Here, the optimal composition found is used and fragments are accelerated by detonation of an explosive charge with the aim to proof intact acceleration of the fragment and proof of reaction at the target.

# 2. Experimental

The preparation of the energetic fragments is described in Lloyd et al. [1]. First the preparation of an assembly with an explosive charge, a casing with liner and energetic fragments is described, followed by the experimental set-up for explosively driven acceleration of the fragments with target plates. Analysis of experiments include scanning electron microscopy with energy dispersive X-ray spectroscopy for elemental analysis (SEM-EDX).

#### 2.1. Assembly of explosive and energetic fragments

The explosive charge consists of Semtex 10, a plastic explosive containing 84.5 wt% PETN, with a density of 1.51 g/cm³. The charge is 30 mm  $\varnothing$  X 100 mm and the enclosure is either a steel housing with 4 mm thick walls, or plastic with 2 mm wall thickness. The fragments are cast in a polydimethylsiloxane rubber (PDMS). A 40 mm entrance and a 30 mm exit section are present along the charge for stable detonation and proper acceleration of energetic fragments. A diagram showing the final experimental set-up is shown in Figure 1.

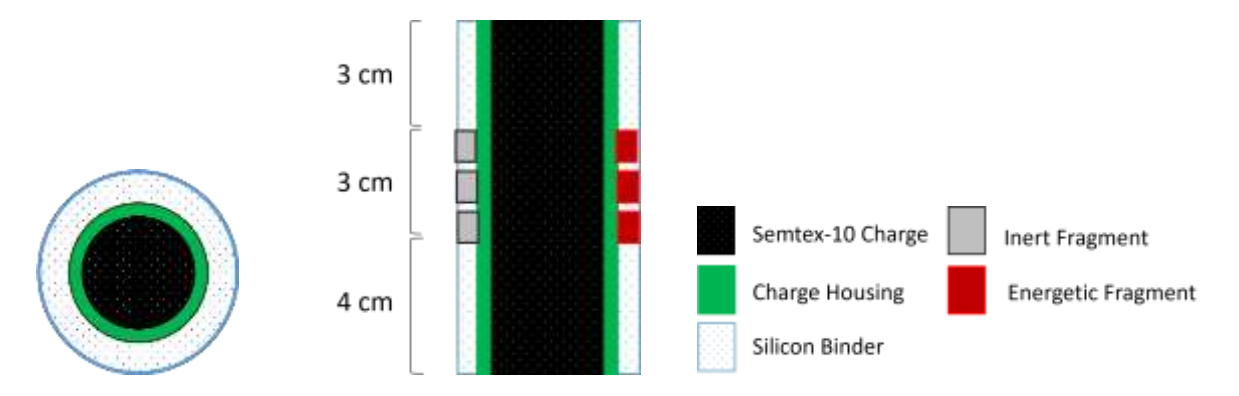


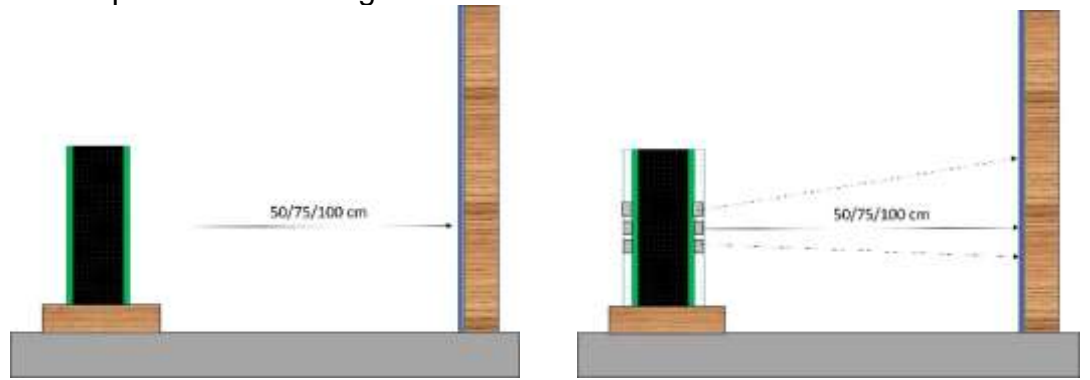
Figure 1 Diagram of charge set-up from above (left) and cross-sectional (middle). Key is provided to aid identification.

Surrounding the centre of the explosive charge are 3 layers of 13 fragments per layer. All fragments are 10 mm  $\oslash$  x 10 mm. Inert fragments (IFs) are solid aluminium. For the energetic fragments (EFs), the chosen formulation is 23EM0099 – an aluminium/bismuth oxide composition that contains 17.5 wt% of soluble fluoropolymer. In the final test configuration, one half of the assembly is comprised of inert fragments, whilst the other half of energetic fragments.

# 2.2. Explosive acceleration test

The experiments are split into three configurations to determine; 1) the fragmentation effect of charge enclosure, 2) the dispersion from inert fragments and 3) the integrity of fragments during explosive acceleration in comparison to inert fragments. The set-

up for each part is noted in Figure 2.



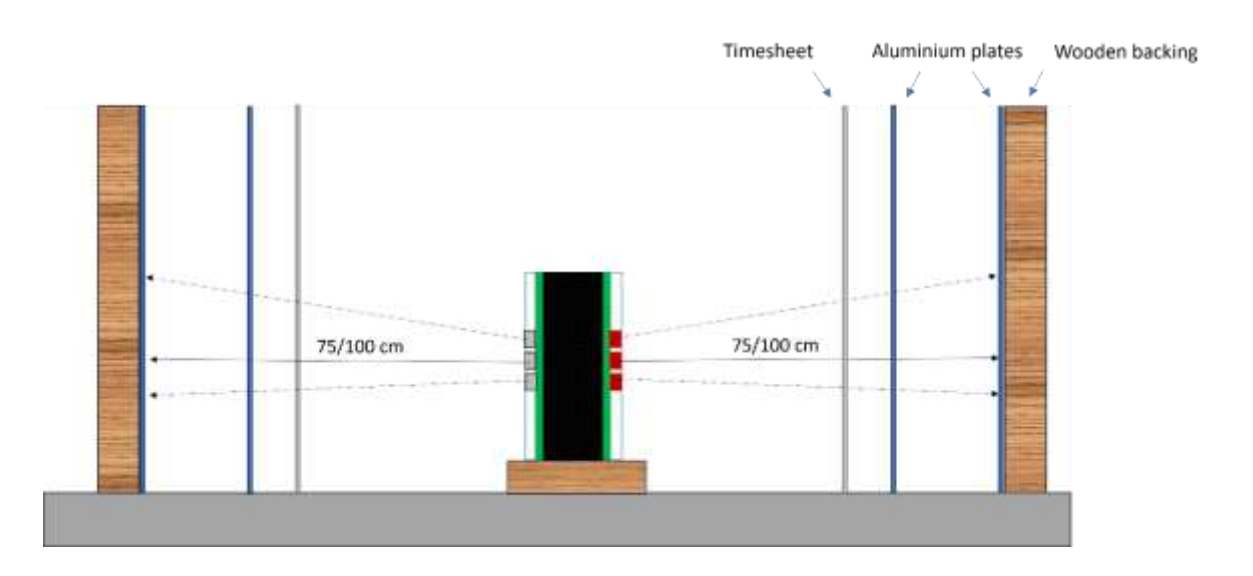


Figure 2 Experimental configurations 1) using "blank" charges (top-left), 2) with only inert fragments (top-right) and 3) half energetic and half inert fragments (bottom).

The enclosure material varies to achieve the desired target velocity. To propel fragments at velocities of approximately 1.0 and 1.5 km/s, the enclosure material is steel and plastic, respectively. The velocities were chosen based on the careful balance between the intact acceleration and passage of the energetic fragment towards and through the first target plate, and secondary reaction upon the back plate. The target comprises aluminium plates measuring  $250 \times 250 \times 2 \, \text{mm}$ , supported with thick wooden plates to capture residual fragments. For configurations 1 and 2, there are 3 target plates positioned 50, 75 and 100 cm from the centre of the charge. In configuration 1, the charge is "bare" with no binder or fragments. In test 1-1 the housing is plastic and 1-2 it is steel. For configuration 2, an initial test with inert aluminium fragments (10 mm  $\varnothing$  X 10 mm), held with silicon binder aimed at verification of penetration of the target plate. Experiments continue to configuration 3 with half IF and half EF. An additional secondary target plate is introduced in configuration of reactive

materials against the rear target plate (shown in Figure 3). Based on configuration 1 and 2, 75 and 100 cm are the selected distances to the back plate in configuration 3.

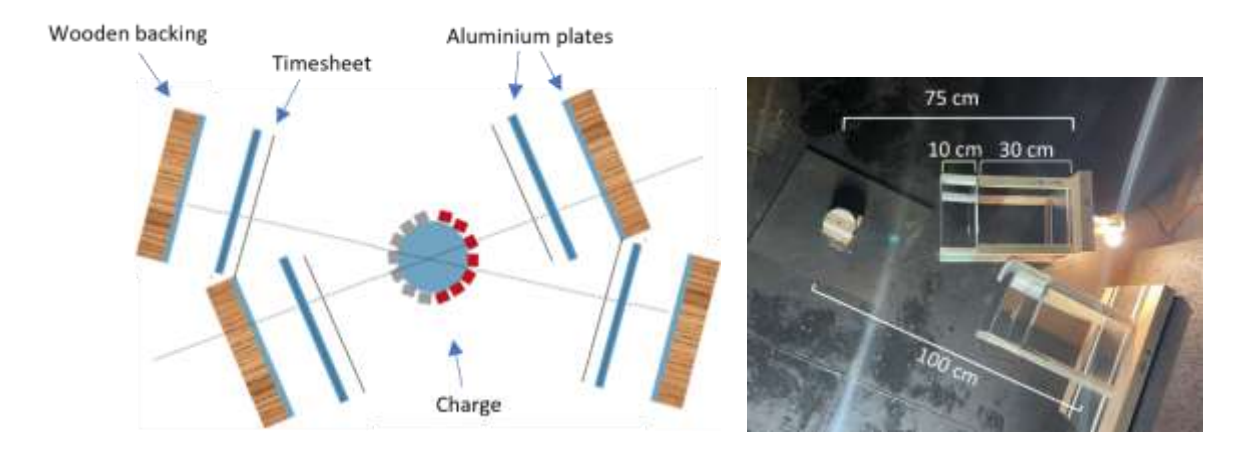


Figure 3 Left: schematic of configuration 3 (not to scale); right: image of the set-up indicating dimensions.

Timesheets are used for configuration 3 to measure the striking and residual velocities of the EF. A timesheet consists of a cardboard frame covered on both sides with aluminium foil. The non-contacting foils are both wired and a voltage difference is imposed. Penetration will cause a short circuit, and the voltage difference will immediately drop, triggering a signal that is displayed at an oscilloscope. The velocity is calculated from the time difference between the triggers from the oscilloscope and the known distance between the timesheets. The distance between the timesheets is 10 cm.

Table 1 Summary of test configurations and parameters.

Test no.	Housing	Inert fragments	Energetic fragments	Distance to target	Secondary target plate	Timesheets
1-1	Plastic 1.5 km/s	-	-	50, 75, 100 cm	-	-
1-2	Steel 1.0 km/s	-	-	50, 75, 100 cm	-	-
2-1	Plastic 1.5 km/s	Yes	-	50, 75, 100 cm	-	-
3-1	Plastic 1.5 km/s	Half	Half	75, 100 cm	Yes	Yes
3-2	Plastic 1.5 km/s	Half	Half	75, 100 cm	Yes	Yes
3-3	Steel 1.0 km/s	Half	Half	75, 100 cm	Yes	Yes
3-4	Steel 1.0 km/s	Half	Half	75, 100 cm	Yes	Yes

#### 3. Discussion and Results

# 3.1. Configuration 1: Fragmentation effect of plastic and steel casing

Initial experiments were carried out as a control "blank" test to determine the fragmentation effect of the plastic and steel liner used in test numbers 1-1 and 1-2, respectively. For the plastic housing the 100 cm target plate showed very little damage, as shown in Figure 4. Single marks and insignificant dents are observed on

target plates located 50 and 75 cm from the charge. In comparison the steel housing resulted in significant damage to the target plates, see Figure 4. Penetration marks of varying sizes and indistinct shapes were noted at all target distances. No soot was observed from the explosive charge.



Figure 4 Target plates at 50, 75, and 100 cm in test number 1-1 with plastic charge housing (top), and test number 1-2 with steel charge housing (bottom).

#### 3.2. Configuration 2: Dispersion from inert fragments

IFs were accelerated using a plastic housing to determine the dispersion pattern from IFs and ensure the correct height of target plates. The use of the plastic housing is beneficial as all penetration marks can be correlated to the inert fragments. The IFs were successfully propelled and reached the targets. Interestingly, it was observed that the layered pattern/array of fragments was witnessed across the plates. The top and bottom row fragments of the charge assembly are aligned above each other, see Figure 5 (left), and so is their impact location, see Figure 5 (right). Furthermore, the number of impacts at the target plate within the opening angle from the charge assembly to the target plate, corresponds with the fraction of the total of fragments on the charge circumference for this opening angle. The vertical dispersion between the three layers of fragments is limited.



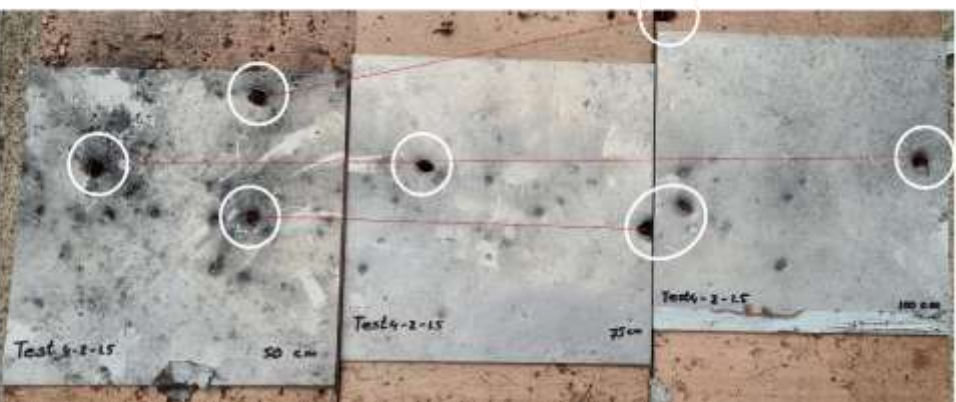


Figure 5 Detail of stacking of aluminium fragments in test number 2-1 (left) and target plates at 50, 75, and 100 cm with indicated impacts of aluminium cylindrical fragments (white circles).

### 3.3. Configuration three: Integrity of explosively driven energetic fragments

In configuration three a direct comparison was made between the impacts resulting from inert and energetic fragments. Some experiments were with a plastic housing and the others with steel. It is noteworthy that heavy steel fragments contribute significantly to impact and penetration marks and therefore the plastic housing yielded more significant results for assessing the mechanical integrity of the energetic fragment in flight (see Figure 4).

Considering the half of the assembly with inert fragments, there were clear perforations on the front and back target plates from the inert fragments at 75 and 100 cm in test number 3-1, see Figure 6 (left). Front plates were bent and there appeared to be soot from the PDMS binder. Perforations were also observed on the back target plates of the energetic fragments. Less or no soot were present on the back plate. Compared to the inert half, the energetic fragments produced no significant perforations in the front plate at 70 cm, i.e., 100 minus 30 cm, whereas several perforations were observed in the front plate at 45 cm, i.e., 75 minus 30 cm. One observed substantial secondary reaction upon the back plate at 75 cm.





Figure 6 Test number 3-1, with front target plates shown at the bottom of each image, and back plates with wood backing at the top. Target plates facing the inert fragments are shown to the left and energetic fragments to the right.

SEM-EDX was performed on soot samples collected from target plates of test number 3-1 to confirm or negate the presence of bismuth oxide upon the plates, see Figure 7. In this test with the plastic housing, any signs of penetration has a stronger chance of being that from an energetic fragment rather than a fragment of steel or inert aluminium. Also the design fragment velocity is the highest (1.5 km/s), and the worst case for the mechanical load that the fragment has to endure.



Figure 7 SEM-EDX sample collection of soot from test number 3-1.

The SEM-EDX analyses are summarized in Table 2. The samples taken from the front plate contained large amounts of bismuth and aluminium that were comparable to those of the unreacted energetic fragment. However, there were much larger amounts of oxygen present which was to be expected in case of a reaction in air. There were lower amounts of silicon, fluorine and carbon observed, which were likely from the fluoropolymer binder within the energetic fragment and of the silicon rubber encapsulating the fragments. Samples from the back plates of the inert fragments and the energetic fragments, were also collected and measured in the SEM-EDX. A significant difference between the plates was the lack of bismuth upon the inert half and the presence of large amounts of bismuth upon the energetic fragment half. This confirms that the energetic fragments remained intact upon arrival at the first plate, penetrated through this plate and that a secondary reaction occurred upon the back plate.

Table 2 SEM-EDX of front and back plates of test number 3-1, and of the unreacted energetic fragment as reference.

Distance (cm)	Fragment Type	Position Target	Elemental Analysis (Weight %)					
Distance (Cili)			C-K	О-К	F-K	AI-K	Si-K	Ві-М
75	Energetic	Front Plate	8	16	5	25	7	36
75	Energetic	Back Plate	9	16	11	31	5	28
75	Inert	Back Plate	21	32	6	21	17	0
-	Unreacted energetic	-	7	4	24	28	0	38

Test number 3-2 is a duplicate of 3-1. There were no large perforations in the "100 cm" front plate, and large perforations in the "75 cm" plate, see Figure 8. One can see secondary reactions upon the back plate at 75 cm. SEM-EDX again confirmed the

presence of bismuth oxide, and soot from just the binder from a wandering or

ricocheted inert fragment is excluded.



Figure 8 Test number 3-2, with front target plates shown at the bottom, and back plates with wood backing at the top (100 cm distance left and 75 cm right). Target plates were facing the energetic fragments.

Timesheets of the tests seem somewhat inconclusive, see Table 3. The plastic charge holder appears to have achieved the 1.5 km/s target velocity. Yet there is a large range 1.1 – 2.0 km/s. It is acknowledged that the timesheets in a few experiments gave unrealistically high velocities, and this is probably due to direct interaction of the (spall) of the explosive blast wave with the timesheets. The steel housing measured lower than predicted, in the range of 590-820 m/s. In many instances the values were unable to be recorded and no measurements were observed. Also, note that in the set-up the timesheets were as close as 35 cm from the centre of the charge for the 75 cm plates and 60 cm for the 100 cm target plates.

Table 3 Measured velocities from timesheets, EF100 (energetic fragment, 100 cm), IF75 (inert fragment, 75 cm).

Test number	EF100 (m/s)	EF75 (m/s)	IF100 (m/s)	IF75 (m/s)
3-1	1500	-	1100	1400
3-2	2000	-	1350	-
3-3	650	1360*	650	590
3-4	820	750	610	770

<sup>\*</sup> This values appears to be unrealistically high and is probably due to direct interaction of the (spall) of the explosive blast wave with the timesheets.

Tests 3-3 and 3-4 with the steel housing are rather inconclusive in comparison to 3-1 and 3-2, due to the difficulty to distinguish penetration of EF compared to plastic. Soot marks were observed, but it was hard to draw a conclusion from this as steel could have penetrated and EF passed through with it. However, it does indicate that the EF survived the acceleration, see Figure 10.





Figure 10 Test 3-3, front target plates are shown at the bottom of the image, back plates with wood backing at the top. Half energetic fragments target plates (left) and inert aluminium fragments (right) and the distance from charge to back plate is 100, 75, 100 and 75 cm from left to right.





Figure 11 Test 3-4, front target plates are shown at the bottom of the image, back plates with wood backing at the top. Half energetic fragments target plates (left) and inert aluminium fragments (right) and the distance from charge to back plate is 100, 75, 100 and 75 cm from left to right..

# 4. Conclusions

In conclusion, this study investigated the behaviour of processed energetic materials upon explosive acceleration. Energetic fragments were made using an alternative fabrication technique that demonstrates scalability potential. These fragments were chosen for comparison with previously gun-launched fragments that remained intact and achieved the impact velocity of 1.0 km/s. During acceleration, the mechanical loads on the energetic fragments are large due to the detonating explosive. In this work, it was found that the energetic fragments successfully survived the explosive

acceleration. The velocities were measured using timesheets. The velocity ranged between 1100-2000 m/s for the plastic housing and 590-820 m/s for the steel housing. Different test configurations were utilized to evaluate the effect of charge housing and fragment distribution, as well as to compare energetic- and inert fragments. It was found that the energetic fragments remained intact upon arrival at the target plate assembly, penetrated the first aluminium plate, and a secondary reaction occurred upon the back plate. This was confirmed with SEM-EDX. Therefore, it is concluded that the energetic fragments produced, using an alternative production method, survived the mechanical loads enacted upon the fragment during explosive acceleration.

#### 5. References

- [1] H.J. Lloyd, B. Meuken, M.Y.K. Hu, M. Zebregs, G. Boone, R.H.B. Bouma, Experimental study on impact-induced reactive material fragments based on fluoropolymers fabricated using alternative methods, 52<sup>nd</sup> International Annual Conference of the Fraunhofer ICT, 27-30 June 2023, Karlsruhe, Germany
- [2] A. Hahma, Reactive structural materials, 16<sup>th</sup> Workshop on Pyrotechnic Combustion Mechanisms, 28-30 June 2021
- [3] R.G. Ames, Energy Release Characteristics of Impact-Initiated Energetic Materials, Mater. Res. Soc. Symp. Proc. Vol. 896 © 2006 Materials Research Society
- [4] Y. Yuan, B. Geng, T. Sun, Q. Yu, H. Wang, Impact-induced reaction characteristic and the enhanced sensitivity of PTFE/Al/Bi2O3 composites, Polymers 2019, 11, 2049
- [5] H. Zhang, H. Wang, Q. Yu, Y. Zheng, G. Lu, C. Ge, Perforation of double-spaced aluminum plates by reactive projectiles with different densities, Materials 2021, 14, 1229
- [6] T.M., Klapötke, Reactive structure materials, Engineering Science and Military Technologies 4(2), 2020
- [7] M. Seidl, Investigations on the impact induced energy release of pyrophoric alloy fragments, 16<sup>th</sup> Workshop on Pyrotechnic Combustion Mechanisms, 28-30 June 2021
- [8] L. Wang, J. Jiang, M. Li, J. Men, S. Wang, Improving the damage potential of W-Zr reactive structure material under extreme loading condition, Defence Technology 17 (2021) 467-477